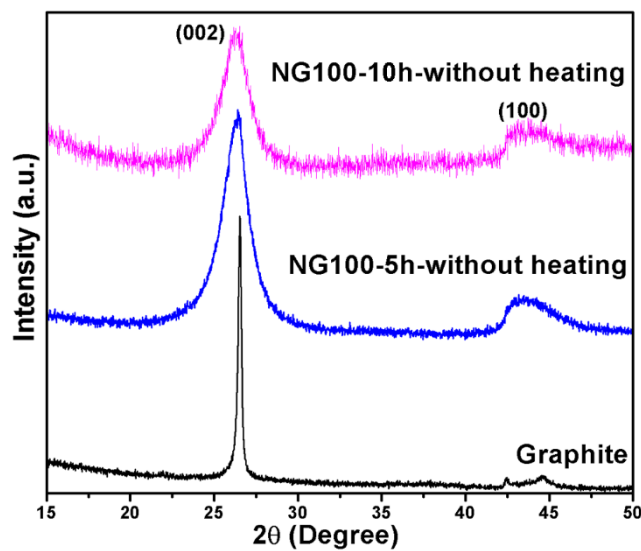


## Supporting Information

### **High N-content holey graphene electrocatalysts: scalable solvent-less production**

*Dan Liu,<sup>a</sup> Weiwei Lei,<sup>\*a</sup> David Portehault,<sup>b</sup> Si Qin<sup>a</sup> and Ying (Ian) Chen<sup>\*a</sup>*



**Figure S1.** Representative XRD patterns of graphite and intermediate products after 5h and 10h milling. To eliminate the effect of the diffraction peaks of GH, both samples were washed by water to remove GH firstly, then freeze dried to avoid the aggregation of graphene layers.

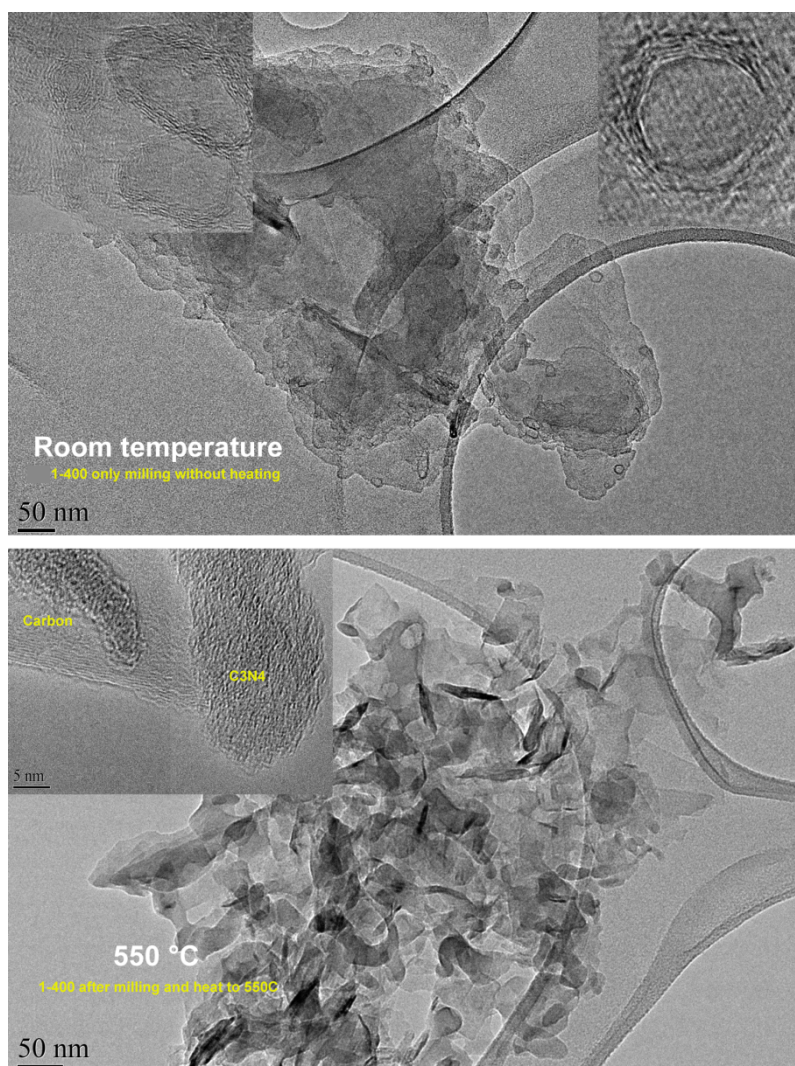


**Figure S2.** TEM pictures corresponding to different heat treatments after milling for the NG400 sample.

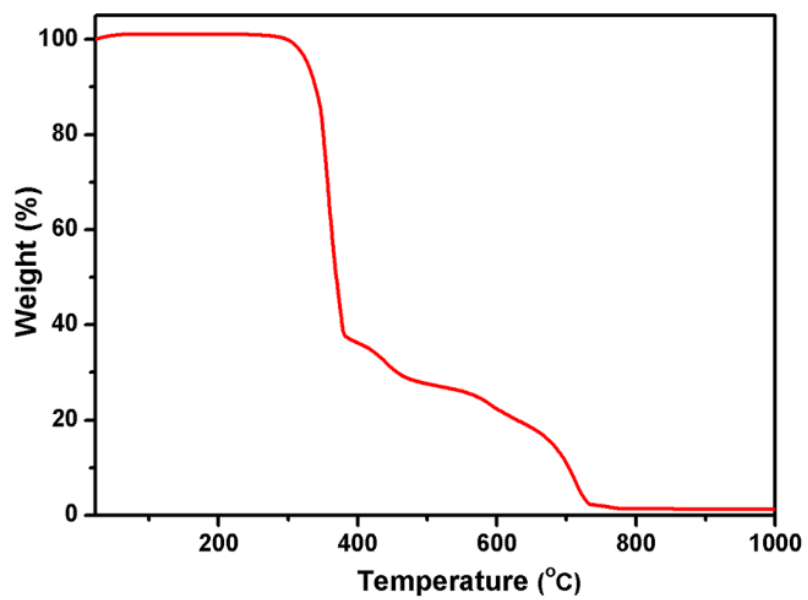


**Figure S3.** TGA analysis of the GH-graphite products.

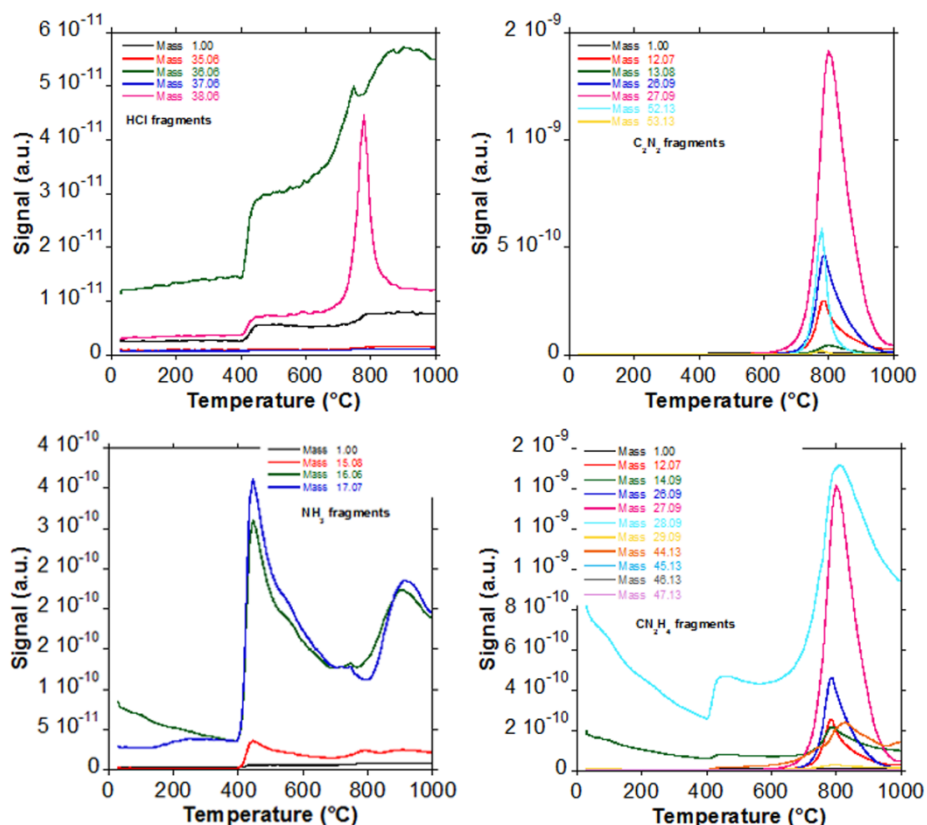


**Figure S4.** Mass spectrometry analysis of the evolved gases monitored by MS-coupled TGA analysis of the thermolysis of NG100. Although  $C_2N_2$  and  $NHCHNH_2$  possess common fragments with cyanides (mass/charge = 27, 28),  $g-C_3N_4$  was not reported to decompose through evolution of HCN (see for instance A. Fischer, *PhD Thesis*, University of Potsdam (Germany), **2008**), so that this gas is strongly unlikely to evolve and the process is considered as safe. Still, for the sake of precautions, a basic water bubbler was connected to the exhaust of the furnace as a trap.

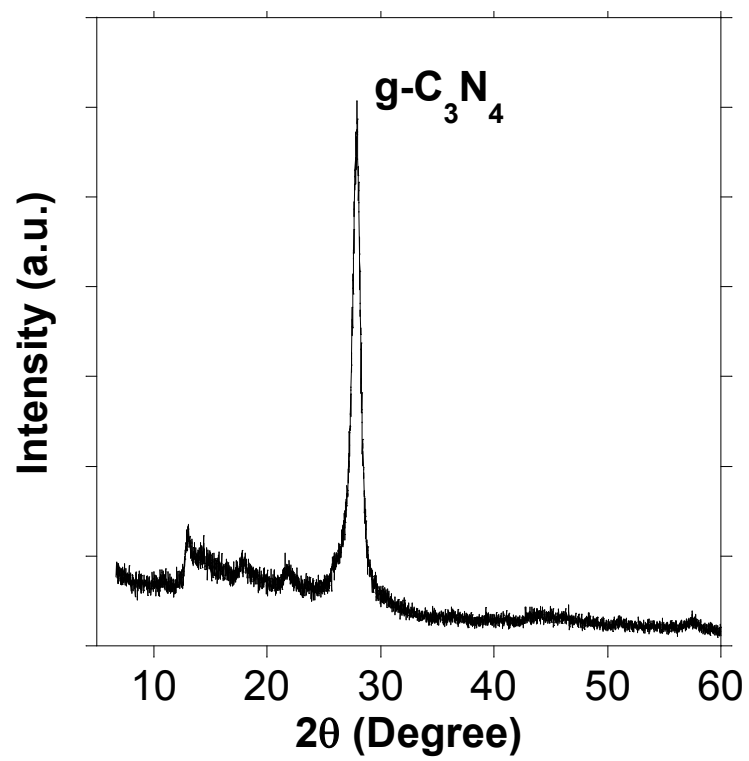


**Figure S5.** XRD pattern of the powder obtained after calcination at 550°C for the NG400 sample.

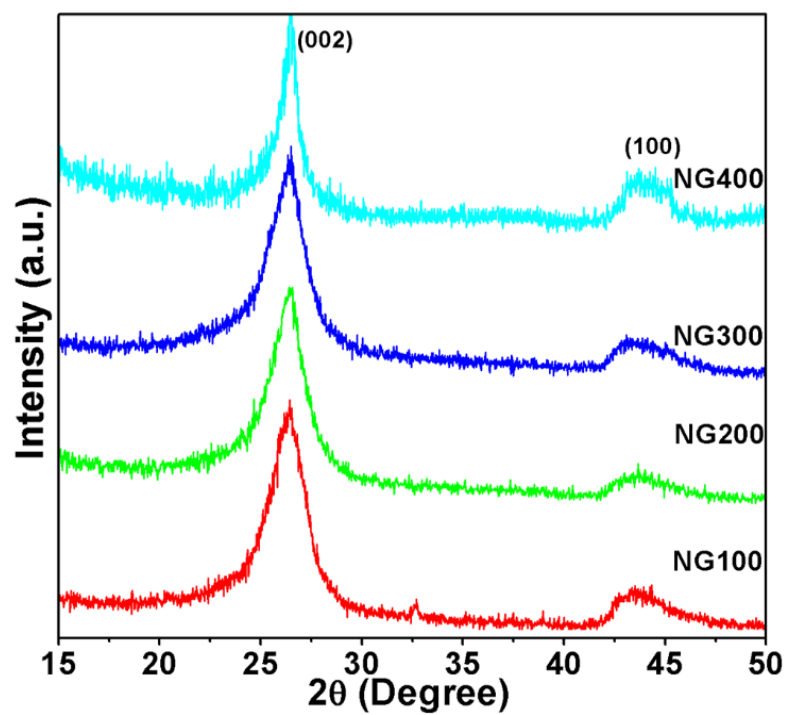
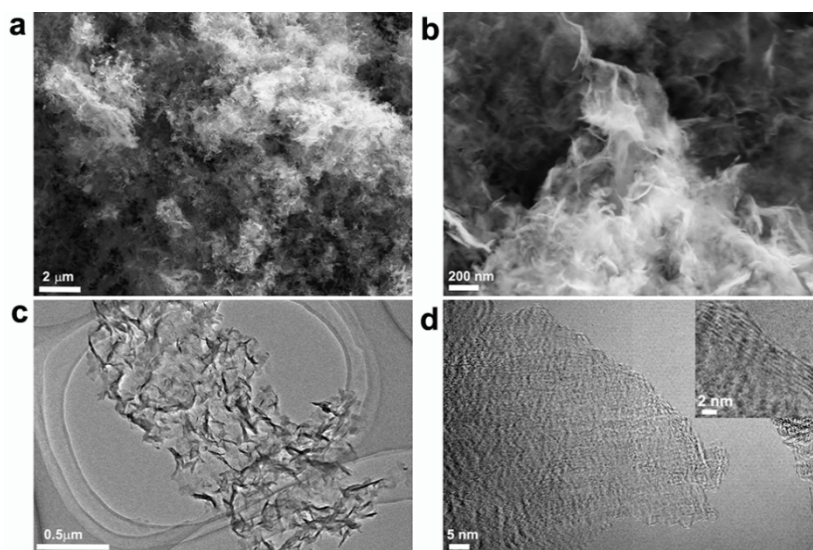
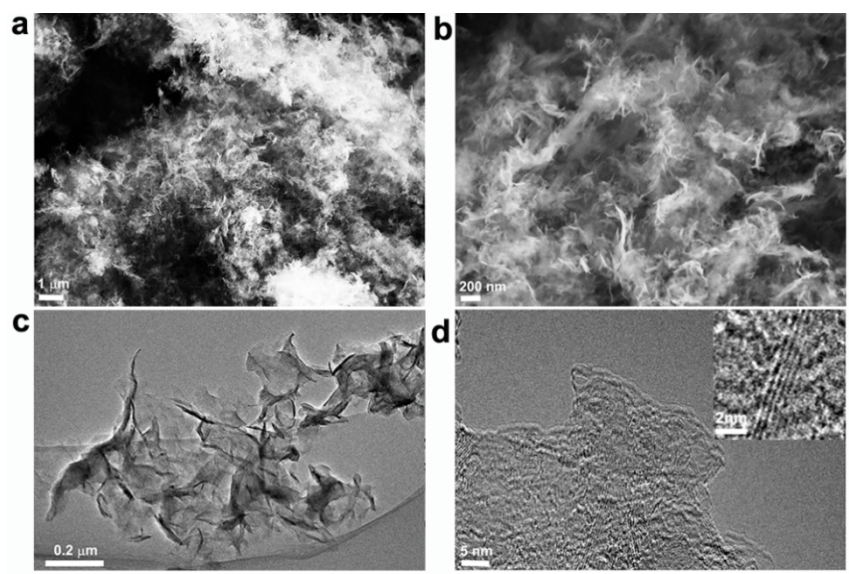


Figure S6. Representative XRD patterns of as-prepared different NG.



**Figure S7.** SEM and TEM images of NG100.





**Figure S8.** SEM and TEM images of NG200.

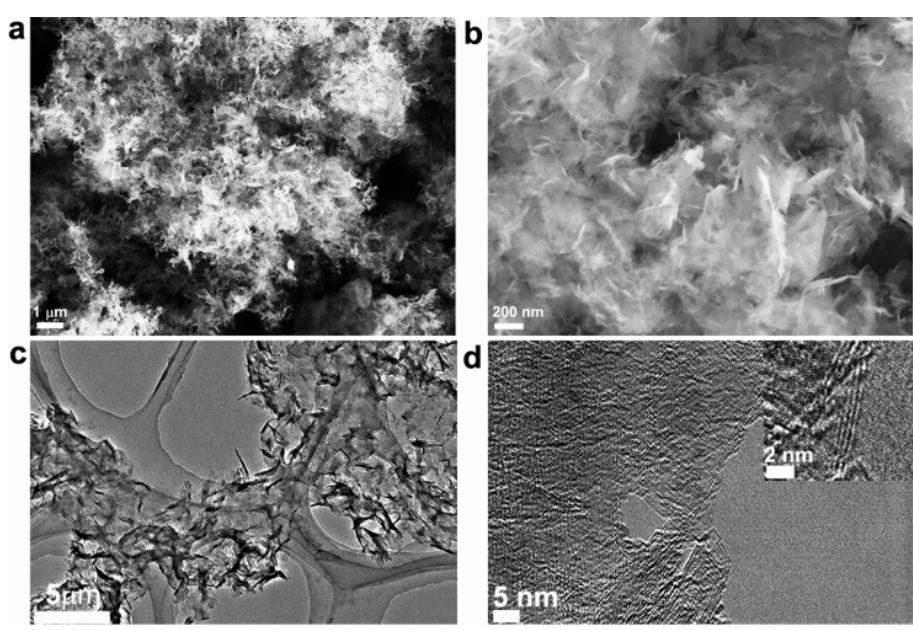


**Figure S9.** SEM and TEM images of NG300.

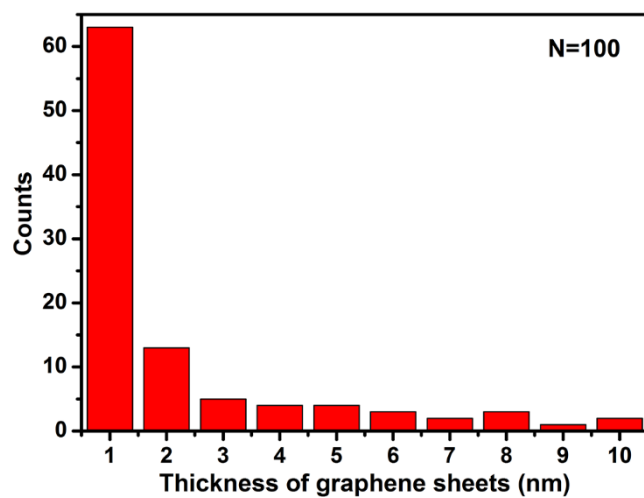


**Figure S10.** Statistical analysis of the thickness for 100 graphene sheets.

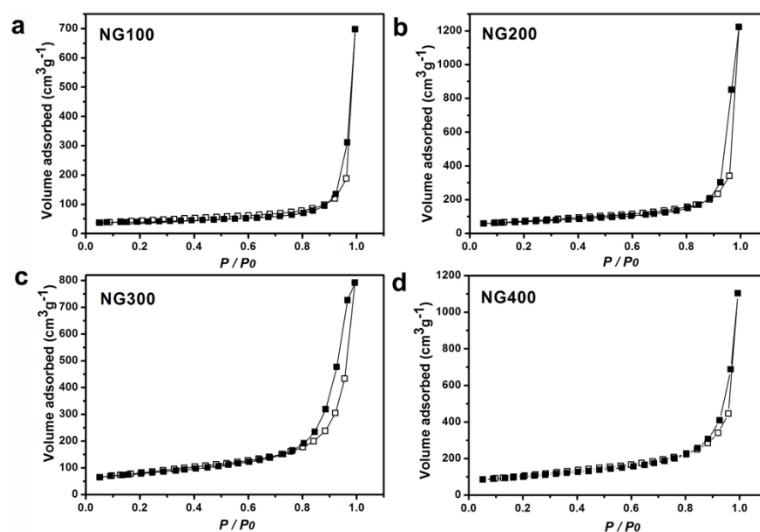


**Figure S11.** Nitrogen adsorption–desorption isotherm of (a) NG100, (b) NG200, (c) NG300, and (d) NG400.

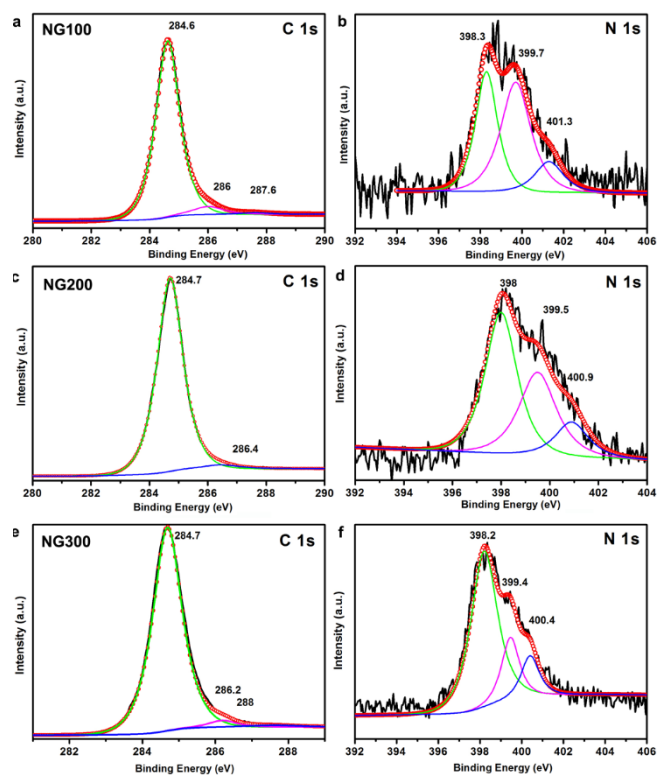


**Figure S12.** High-resolution C1s and N1s XPS spectra of NG100, NG200, and NG300.

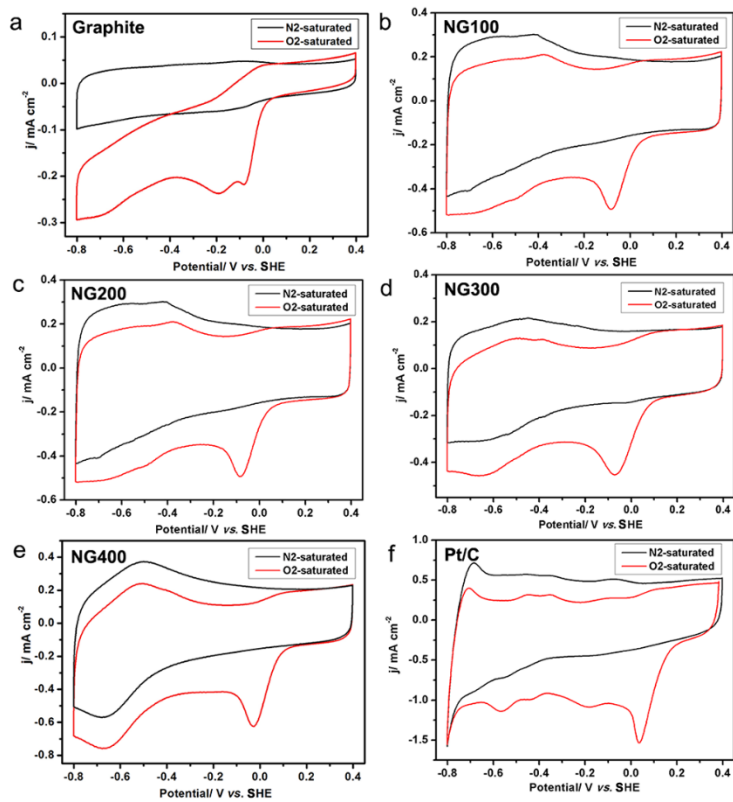


**Figure S13.** Cyclic voltammogram of samples on glassy carbon (GC) electrodes with a scan rate of  $50 \text{ mV s}^{-1}$   $\text{N}_2$ -saturated and  $\text{O}_2$ -saturated  $0.1 \text{ M KOH}$  solution, respectively.

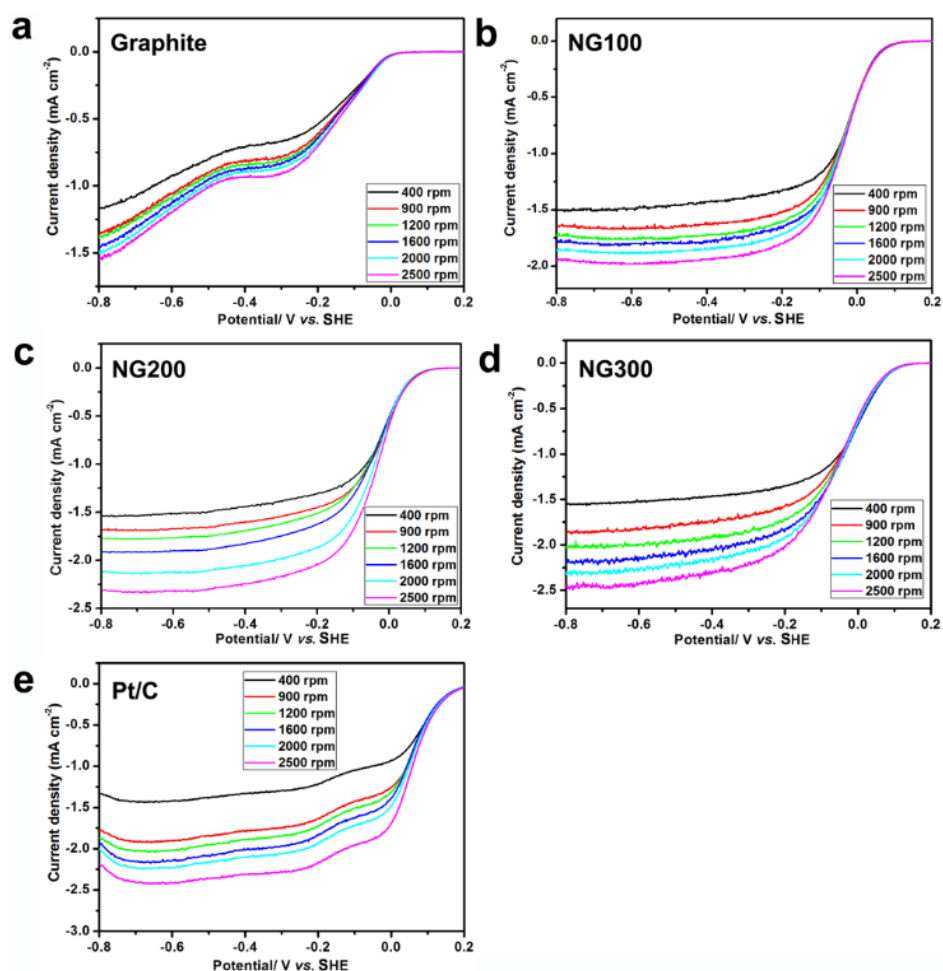
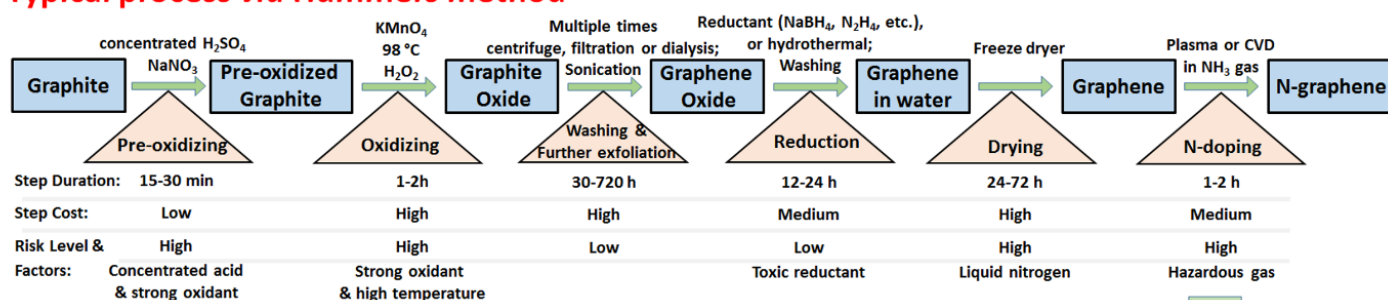


**Figure S14.** Rotating disk electrode (RDE) linear sweep voltammograms of graphite, NG100, NG200, NG300 and Pt/C in  $\text{O}_2$ -saturated  $0.1 \text{ M KOH}$  with various rotation rates at a scan rate of  $5 \text{ mVs}^{-1}$ .

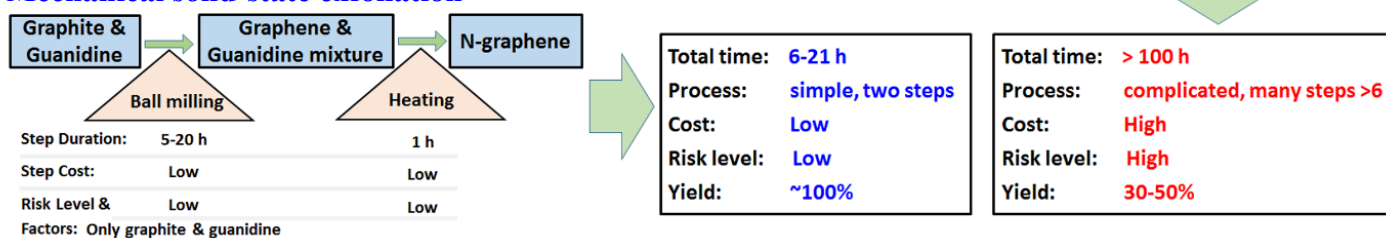
## Yield and simplicity of the mechanical solid-state exfoliation compared to the popular Hummer's method.

The yield versus the limiting reagent (graphite) is ca. 99%. It is higher than the typical solvent-based Hummer's method, with usual rate of 30-50%. As to simplicity and facility, the reported mechanochemical method is solvent-less and uses cheap, harmless reagents. Mechanical solid-state exfoliation compares favourably to the common synthesis methods of graphene and N-doped graphene (Ref 1-9 in the main text), especially, the chemical reduction of graphite oxide method, so called Hummer's method. The latter usually involves strong, hazardous oxidizing reagents (e.g.,  $\text{KMnO}_4$  and  $\text{H}_2\text{SO}_4$ ), hazardous reducing reagents (e.g.,  $\text{NaBH}_4$ ), solvents, excessive sonication and centrifugation, a complicated multistep process requiring 100h to be completed, compared to 24h in our case. In addition, most of further works on N-doped graphene also start from the Hummer's method (Refs 10-13) which then imposes the same limitations. A schematic diagram is provided below to compare both processes.

### Typical process *via* Hummers method



### Mechanical solid-state exfoliation



Scheme 1. Comparison of the Hummer's method and mechanical solid-state exfoliation

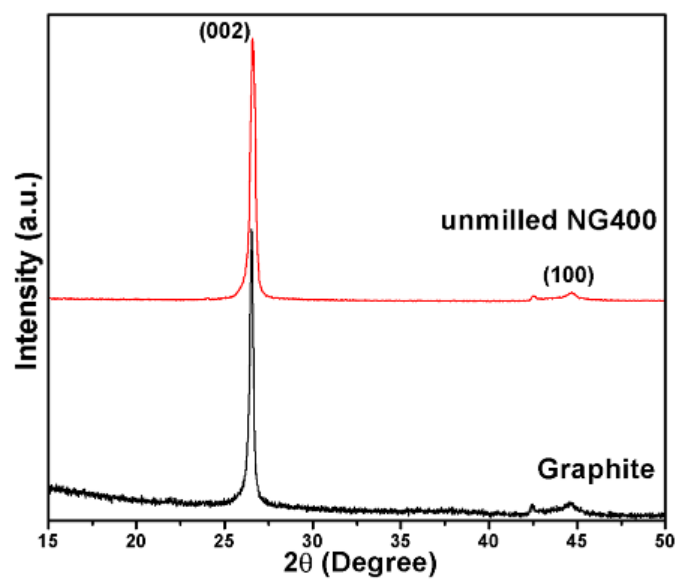


**Figure S15.** The XRD patterns of graphite and unmilled NG400.

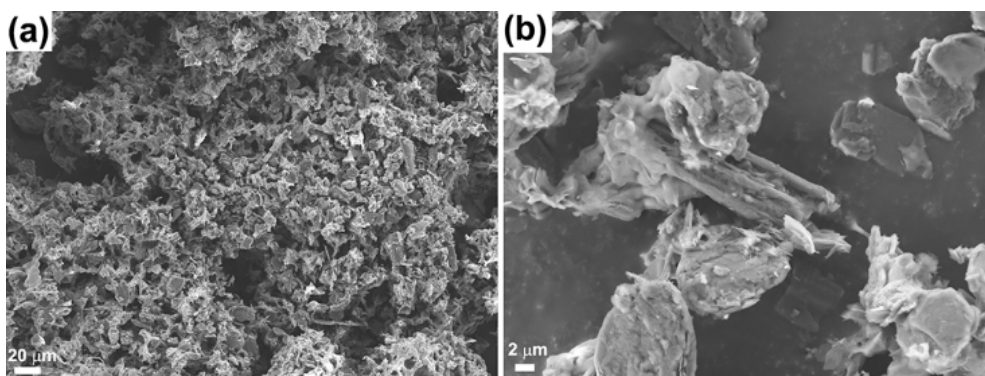


**Figure S16.** SEM images of unmilled NG400.

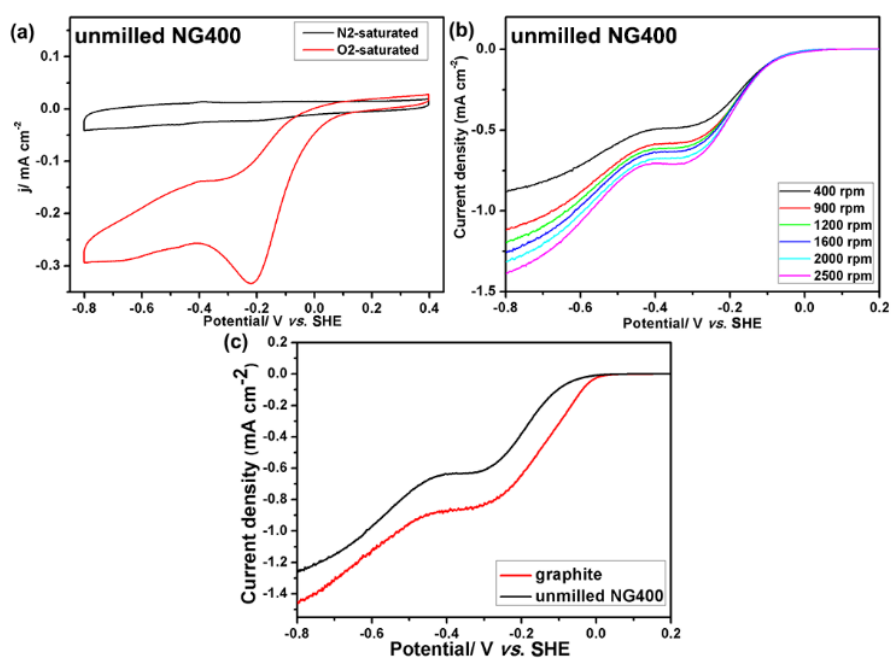


**Figure S17.** (a) Cyclic voltammogram, and (b) Rotating disk electrode (RDE) linear sweep voltammograms of unmilled NG400 on glassy carbon (GC) electrodes with a scan rate of  $50 \text{ mV s}^{-1}$   $\text{N}_2$ -saturated and  $\text{O}_2$ -saturated  $0.1 \text{ M KOH}$  solution. (c) RDE voltammograms of graphite and unmilled NG400 at a rotation rate of  $1600 \text{ rpm}$ .